

# Glass Transition Temperature of Colloidal Polystyrene Dispersed in Various Liquids

Dane Christie,<sup>1</sup> Chuan Zhang,<sup>1</sup> Jie Fu,<sup>2</sup> Bruce Koel,<sup>1,2</sup> Rodney D. Priestley<sup>1,3</sup>

<sup>1</sup>Department of Chemical and Biological Engineering, Princeton University, Princeton, New Jersey 08544

<sup>2</sup>Department of Chemistry, Princeton University, Princeton, New Jersey 08544

<sup>3</sup>Princeton Institute for the Science and Technology of Materials, Princeton University, Princeton, New Jersey 08544

Correspondence to: R. Priestley (E-mail: rpriestl@princeton.edu)

Received 24 February 2016; accepted 19 April 2016; published online 20 May 2016

DOI: 10.1002/polb.24082

**ABSTRACT:** Recently, there has been significant interest in measuring the glass transition temperature ( $T_g$ ) of thin polymer films floated atop liquid substrates. However, such films still have intrinsically asymmetric interfaces, that is, a free surface and a liquid–polymer interface. In an effort to analyze the influence of different liquids on the  $T_g$  of confined polymers in which there is no interfacial asymmetry, a colloidal suspension of polystyrene (PS) nanoparticles (NPs) was employed. The  $T_g$ s of PS NPs suspended in either glycerol or an ionic liquid were characterized using differential scanning calorimetry. Nanoparticles suspended in an ionic liquid showed an invariance of  $T_g$  with confinement, that is, decreasing diameter. In contrast, nanoparticles suspended in glycerol showed a slight decrease

in  $T_g$  with confinement. The dependence of NP  $T_g$  on the nature of the surrounding liquid exhibited a positive correlation with the interfacial energy of the liquid–PS interface and no correlation with interfacial softness, as measured by viscosity. A comparison of the results with thin films supported by liquid or solid substrates revealed a nontrivial interplay between interfacial softness and interfacial interactions on the  $T_g$  of confined PS. © 2016 Wiley Periodicals, Inc. *J. Polym. Sci., Part B: Polym. Phys.* **2016**, *54*, 1776–1783

**KEYWORDS:** calorimetry; confinement; glass transition; interfacial energy; nanoparticles

**INTRODUCTION** The glass transition temperature ( $T_g$ ) is a critical parameter in the characterization of amorphous polymers and can be strongly influenced by molecular parameters, for instance, molecular weight<sup>1</sup> and tacticity<sup>2</sup> as well as processing conditions<sup>3</sup> due to its kinetic manifestation at laboratory time-scales. For the past two decades, there has been growing evidence that with physical confinement to the nanometer length scale, the  $T_g$  of polymer thin films can deviate dramatically from the bulk.<sup>4–14</sup> The seminal work of Keddie et al. in 1994 suggested that the size-dependent  $T_g$  of spin-coated polymer thin films was attributed to the presence of interfacial effects that acted to locally modify glassy dynamics.<sup>15</sup> In their initial investigations, in which ellipsometry was used to measure the  $T_g$  of polystyrene (PS) and poly(methyl methacrylate) (PMMA) films supported on silicon wafers, a non-universal trend was observed, in which PS exhibited a suppressed  $T_g$ , while PMMA showed an enhanced  $T_g$  with decreasing film thickness.<sup>16</sup> In supported films, interfacial effects would arise from the polymer–substrate interface as well as the free surface. There is a growing literature consensus that the depression in  $T_g$  of PS films supported by a non-interacting substrate (i.e., silicon wafer) originates from the free surface due to a

layer of enhanced mobility, which itself has a reduced  $T_g$ .<sup>17–28</sup> In contrast, the  $T_g$  enhancement in PMMA films supported on silicon wafers, in which interfacial interactions exist, originates from a competition between free surface and substrate effects. In essence, the substrate that acts to reduce local dynamics overwhelms free surface effects and results in an overall increase in the  $T_g$  of the film with confinement.<sup>29–33</sup>

Supported films have intrinsic interfacial asymmetry, that is, a free surface and a substrate-interface, which adds complexity to understanding confined glassy properties. To overcome this issue, researchers have undertaken studies on freestanding or doubly supported films. Dutcher et al. reported that in the absence of a solid interface, that is, the freestanding film geometry, PS and PMMA exhibited a depression in  $T_g$  with decreasing film thickness.<sup>34,35</sup> Conversely, PS films that were doubly supported by aluminum or silica, that is, those with no free surface, exhibited a size-independent  $T_g$  with confinement.<sup>25,36</sup> Combined, these reports provide evidence that changes in  $T_g$  of polymer films with confinement are directly correlated to the presence or lack of free and solid interfaces.

Recently, there has been a growing interest in measuring the  $T_g$  of polymer thin films floated atop liquids. This motivation stems from the fact that thin films prepared by spin coating are meta-stable with respect to polymer chain conformations, and that it is unclear whether high temperature ( $T > T_g$ ) annealing of thin films supported on solid substrates can lead to equilibration.<sup>37–40</sup> The idea is that a “soft” liquid substrate could facilitate a greater extent of chain equilibration after film casting in comparison to films supported on solid substrates.

In 2007, Bodiguel and Fretigny reported only a slight reduction in the  $T_g$  of PS films floated atop glycerol by monitoring the change in the shape of the film due to dewetting. For instance, a 3 K reduction in the  $T_g$  was observed for a 20 nm thick PS film.<sup>39</sup> Subsequently, Lu et al. employed an optical-based approach to measure the  $T_g$  of PS thin films floated atop four different ionic liquids. They observed a size dependence of the “kink” temperature of thin PS films floated atop ionic liquids, including 1-butyl-3-methylimidazolium trifluoromethanesulfonate ([BMIM][CF<sub>3</sub>SO<sub>3</sub>]).<sup>37</sup> They cautioned that the kink temperature should not be considered as the  $T_g$  since the measurements were not performed at equilibrium conditions. Applying an experimental protocol similar to the Bodiguel–Fretigny dewetting method, but allowing for the measurement of  $T_g$  for multiple thicknesses in a single film, McKenna et al. also observed a reduction in  $T_g$  of PS films floated atop glycerol, albeit to a greater extent than that reported earlier.<sup>40</sup> A slightly more pronounced size-dependent  $T_g$  was observed for PS films floated atop ionic liquids, including ([BMIM][CF<sub>3</sub>SO<sub>3</sub>]), that is, the same ionic liquid study by Lu et al.<sup>37</sup> Despite the caution by Lu et al.,<sup>37</sup> when McKenna et al.<sup>41</sup> equated the size-dependent kink temperature of PS to  $T_g$ , a good agreement was observed between the two studies.

While the above studies were partially designed to minimize the influence of residual stresses induced during spin coating on the measurement of the thin film  $T_g$ , they also highlighted the need to further investigate the role liquid media has on the properties of confined polymers. Unfortunately, thin films have intrinsically asymmetric interfaces when floated atop of liquids, that is, a free surface and liquid–polymer interface. Such interfacial asymmetry brings about complexity, reminiscent of substrate-supported thin films. This is because the two different interfaces may modify glassy dynamics in a different manner and make it difficult to characterize substrate-specific effects on  $T_g$ . The ability to perform size-dependent  $T_g$  studies in which only one liquid interface exists would simplify the interactions that modify  $T_g$ . Here, we aim to address this challenge.

Previously, we have demonstrated the ability to measure  $T_g$  of colloidal PS dispersed in an aqueous medium.<sup>42</sup> The  $T_g$  was measured via differential scanning calorimetry (DSC). It was demonstrated that the  $T_g$  of PS nanoparticles decreased when the diameter was less than approximately 400 nm. Such observation was in quantitative agreement with measurements performed on freestanding films of PS when compared via a characteristic size scale, that is, the volume to

surface area ratio. An advantage of investigating nanoparticles dispersed in a liquid medium is that they have intrinsically only one interface, thus providing a unique opportunity to further our understanding of the role of confinement on the  $T_g$  in the presence of different liquids. Another advantage of performing studies on nanoparticles, as opposed to thin films, is that the former is processed in a very different manner. Hence, they provide an indirect means to assess the influence of residual stresses induced during processing on confined glassy properties. Finally, nanoparticles suspended in solutions may be annealed above  $T_g$  for prolonged periods of time for equilibration to remove residual stresses to the greatest extent possible. Reference 43 provides a detailed review on the current state of confined glassy properties of polymer nanoparticles.

In this study, we measured the  $T_g$  of colloidal PS dispersed in various liquid media, for example, glycerol and ionic liquid, via DSC. In all cases, the liquids were thermally stable in the temperature range of interest and did not swell or dissolve PS. We observed only a slight decrease in the  $T_g$  of PS nanoparticles with decreasing diameter when dispersed in glycerol. In contrast, a size-invariant  $T_g$  of the PS nanoparticles was observed when dispersed in the ionic liquid. We discuss both the influence of interfacial softness, as measured by viscosity, and interfacial interactions, as measured by surface energy, on the observed trends. Comparisons are also made with literature studies of thin films floated atop liquids as well as supported atop chemically treated silicon wafers. Our findings suggest a complex interplay between the role of interfacial softness and interfacial interactions on the  $T_g$  of nanoconfined PS.

## EXPERIMENTAL

### Nanoparticle Synthesis

Uniform bare PS nanoparticles were synthesized from surfactant-free emulsion polymerization, as described previously.<sup>44–46</sup> In a typical synthesis, 0.037 g of ammonium persulfate (98%, Sigma-Aldrich) was initially added to 100 mL of deionized (DI) water in a three-neck flask. The solution was bubbled with nitrogen for approximately 20 min and then heated to 348 K. Subsequently, 5 g of deionized styrene ( $\geq 99\%$ , Sigma-Aldrich) was combined with 0.05 g of acrylic acid (99%, Sigma-Aldrich), and the mixture was injected into the flask. The solution was then allowed to polymerize under reflux conditions for 20 h. After polymerization, the resulting suspension was washed at least three times by centrifugation and ultimately suspended in DI water. Nanoparticle diameter ( $d$ ) was controlled by changing the starting concentrations of styrene, ammonium persulfate, and acrylic acid. The addition of a small amount of acrylic acid ( $< 5$  wt% with respect to styrene for all nanoparticle samples) as a co-monomer provided stability to the colloidal suspension.

### Preparation of Dispersions

In order to suspend PS nanoparticles of varying diameters into glycerol or the ionic liquid, a portion of the surfactant-

free emulsion polymerized PS nanoparticles originally suspended in water was mixed with either glycerol ( $\geq 99.5\%$ , Sigma-Aldrich) or [BMIM][CF<sub>3</sub>SO<sub>3</sub>] ( $\geq 95\%$ , Sigma-Aldrich). Subsequently, PS nanoparticles suspended in a water/glycerol or water/ionic liquid environment were dried in a vacuum oven for at least 3 days. Due to the low vapor pressures of glycerol and the ionic liquid, vacuum drying the PS nanoparticles suspended in these mixed liquids resulted in the removal of only the water. Thus, after 3 days of vacuum drying (i.e., water removal), the PS nanoparticles were suspended in either pure glycerol or [BMIM][CF<sub>3</sub>SO<sub>3</sub>]. Particles suspended in either glycerol or [BMIM][CF<sub>3</sub>SO<sub>3</sub>] could be re-dispersed in an aqueous environment via continued dilution. We note that bulk polymer was prepared from PS NPs suspended in water by drying and then annealing at 423 K for 20 h.

### Characterization

The sizes of PS nanoparticles suspended in H<sub>2</sub>O were determined from dynamic light scattering (DLS) (Malvern Instruments Zetasizer Nano-ZS ZEN 3600). Weight-average molecular weight ( $M_w$ ) of each nanoparticle sample in tetrahydrofuran was determined from gel permeation chromatography (GPC) (Waters 515 HPLC pump, Eppendorf CH-460 column heaters, Waters 410 differential refractometer). The  $T_g$ s of PS nanoparticles suspended in either glycerol or water were determined using DSC (TA Instruments Q2000, second heat with a heating rate of 10 K/min) in hermetically sealed aluminum pans. All reported  $T_g$ s are the midpoint value between the tangents of the glass and liquid line from the total heat flow. We have previously shown in prior works,<sup>42,47</sup> as well as by others,<sup>48,49</sup> that the nanoparticles do not agglomerate but remain dispersed during the measurement of  $T_g$ . X-ray photoelectron spectroscopy (XPS) measurements were performed in an ultrahigh vacuum (UHV) system with  $2.0 \times 10^{-10}$  torr base pressure. Al K $\alpha$  X-rays (1486.6 eV; PHI 04-548 dual anode X-ray source) and a hemispherical energy analyzer (SPECS PHOIBOS 100-5 MCD) were used to investigate the surface fluorine concentrations of PS NPs re-suspended from [BMIM][CF<sub>3</sub>SO<sub>3</sub>]. F 1s XPS spectra were obtained at 20 eV pass energy and the analyzer normal to the surface.

## RESULTS AND DISCUSSION

### $T_g$ of Polystyrene Nanoparticles Suspended in Glycerol or Ionic Liquid

Figure 1(A) shows representative DSC thermograms of PS nanoparticles of various diameters ranging from 110 to 428 nm dispersed in [BMIM][CF<sub>3</sub>SO<sub>3</sub>]. The inset in Figure 1(A) shows the chemical structure of the ionic liquid. As evident from the curves, the  $T_g$  of the PS nanoparticles does not systematically deviate from the bulk  $T_g$  with decreasing diameter. Figure 1(B) shows representative DSC thermograms of PS nanoparticles of various diameters suspended in glycerol. The inset shows the chemical structure of glycerol. In contrast to the size-invariant  $T_g$  observed for PS nanoparticles suspended in the ionic liquid, those suspended within

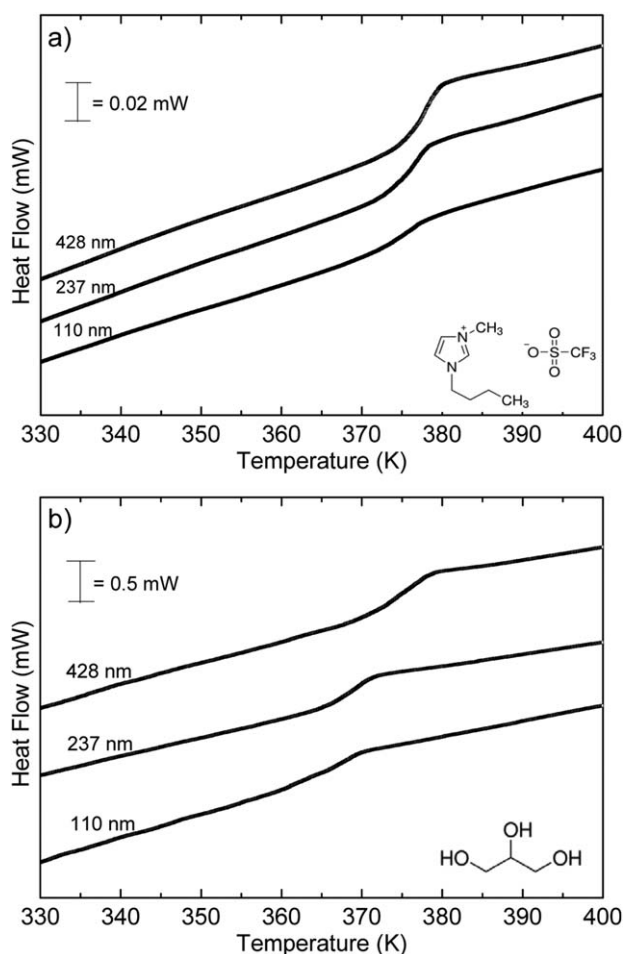


**FIGURE 1** (a) Calorimetric thermograms of PS NPs of various sizes suspended in [BMIM][CF<sub>3</sub>SO<sub>3</sub>]. Inset, chemical structure of [BMIM][CF<sub>3</sub>SO<sub>3</sub>]. (b) Calorimetric thermograms of PS NPs of various sizes suspended in glycerol. Inset, chemical structure of glycerol.

glycerol show a size-dependent  $T_g$ . For particles with  $d > 600$  nm,  $T_g$  is approximately 378 K irrespective of the dispersing media and is identical to bulk  $T_g$ . However, for smaller particles the dispersing medium has a strong influence on the  $T_g$ . We note that the  $M_w$  of the polymers, as measured by GPC, are between approximately 120 and 350 kg/mol, and that there is a tendency for the larger NPs to have a greater molecular weight due to the mechanism of emulsion polymerization.

Figure 2(A) shows the diameter dependence of  $T_g$  for PS nanoparticles dispersed in [BMIM][CF<sub>3</sub>SO<sub>3</sub>] and glycerol over the complete size range investigated. The trend observed for particles suspended in [BMIM][CF<sub>3</sub>SO<sub>3</sub>] is an invariance of  $T_g$  with confinement. For particles suspended in glycerol, a decrease in  $T_g$  with increasing confinement is observed. For PS particles in glycerol, the onset diameter for the reduction in  $T_g$  is approximately 400 nm. We note that the error bars represent the standard deviation from three measurements.

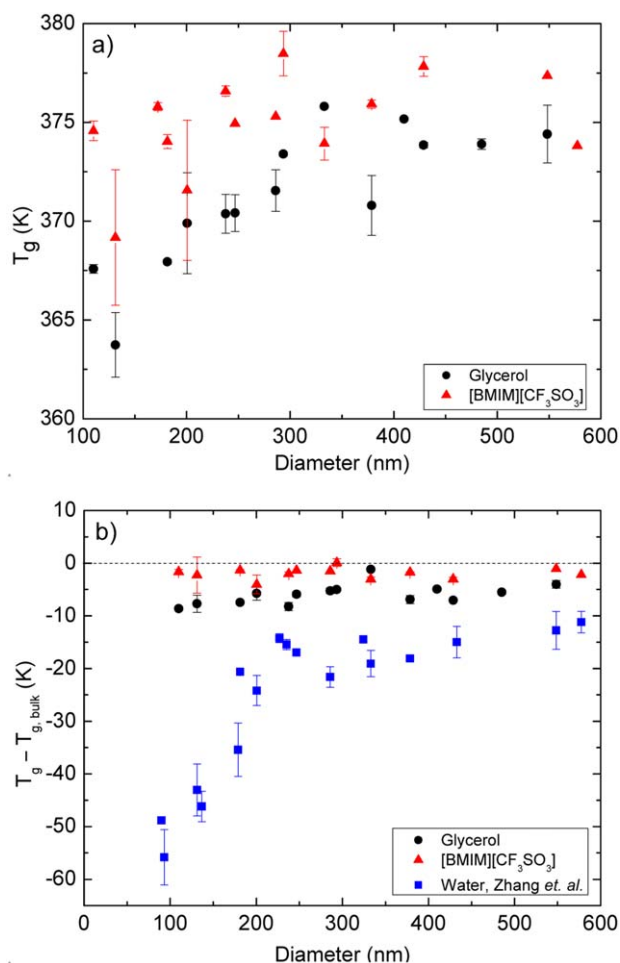


**FIGURE 2** (a) Size dependent  $T_g$  of PS NPs suspended in glycerol and [BMIM][CF<sub>3</sub>SO<sub>3</sub>]. (b) Size dependent  $T_g$  shift ( $T_g - T_{g,bulk}$ ) of PS NPs suspended in glycerol, [BMIM][CF<sub>3</sub>SO<sub>3</sub>], and water from Zhang et al. (ref. 42). [Color figure can be viewed in the online issue, which is available at [wileyonlinelibrary.com](http://wileyonlinelibrary.com).]

In Figure 2(B), we plot the  $T_g - T_{g,bulk}$  for PS NPs suspended in [BMIM][CF<sub>3</sub>SO<sub>3</sub>] and glycerol. We also plot the  $T_g$  deviation of PS NPs suspended in water from our prior study utilizing the same experimental protocol.<sup>42</sup> Clearly, for the PS NPs employed in this investigation, the dispersing medium has an influence on the deviation of  $T_g$  with decreasing diameter. The NPs exhibited an invariant, weak, and strong dependence of the  $T_g$  shift with confinement when suspended in [BMIM][CF<sub>3</sub>SO<sub>3</sub>], glycerol, and water, respectively. To the best of our knowledge, this is the first observation in which the dispersing medium has been shown to strongly influence the  $T_g$  of PS NPs.

### Role of Interfacial Softness on $T_g$ Deviation of PS Nanoparticles

In a prior work, we demonstrated that the  $T_g$  deviation of PS NPs agreed quantitatively with those of PS freestanding films when compared via a characteristic size, that is, the volume to surface area ratio, despite the difference in the fact that the  $T_g$  for films was measured in an air environment while

that of NPs was measured in an aqueous environment. We classified both interfaces (water-PS and air-PS) as “soft” because of their low viscosities in comparison to the polymer. The consistency between the size-dependent  $T_g$  of PS NPs and thin films pointed to a similar influence of the two interfaces in enhancing the glassy dynamics of confined polymers.

Here, in the same context, the current findings may be rationalized in terms of the enhanced mobility of glassy dynamics at the liquid-polymer interface. It would then follow that the segmental dynamics at the liquid-PS interface would be enhanced in comparison to the bulk in the following order: water > glycerol > [BMIM][CF<sub>3</sub>SO<sub>3</sub>], in accordance with the magnitude of the observed  $T_g$  depressions.

One possible origin for the observed trends is due to differences in the “softness” of the liquids in terms of their viscosities. With respect to PS, a softer interface would facilitate enhanced interfacial dynamics. Previously, it has been demonstrated that PS NPs capped with a rigid shell exhibited no size-dependent  $T_g$ <sup>42</sup> while those dispersed in a rubbery matrix exhibited a weak size-dependent  $T_g$ .<sup>50</sup> Furthermore, recent studies on stacked multilayer films, including PS layers, also revealed a strong influence of the interfacial softness on the confined  $T_g$  via fluorescence.<sup>51</sup> For the liquids employed in this investigation, the order of viscosity is as follows: glycerol > [BMIM][CF<sub>3</sub>SO<sub>3</sub>] > water. The order of the increase in softness, as measured by viscosity, is different from the order of the  $T_g$  depression of PS NPs dispersed in the various liquids. Hence, for PS nanoparticles employed in this investigation, interfacial softness alone cannot be used to describe the observed trends.

One argument for the lack of correlation between the interfacial softness and the magnitude of the  $T_g$  depression observed for PS NPs is that viscosity is not the appropriate metric for softness. *A priori*, there is no reason why this should not be the case. However, recently Simmons and coworkers have performed a series of molecular dynamics simulations on stacked multilayer polymer films. In their investigation, the  $T_g$  of one layer was measured as a function of the stiffness of two adjacent layers. The stiffness was quantified by the ratio of each layer’s Debye-Waller factor. An exponential correlation between the magnitude of the  $T_g$  deviation and stiffness was observed, thus allowing for the construction of an empirical expression that related  $T_g$  deviations to the stiffness of the confining matrix.<sup>52</sup> Unfortunately, reliable values of the Debye-Waller factor for the liquids employed in the investigation and for the appropriate temperature range are not available. Hence, we are unable to confirm any correlation (or lack thereof) between the magnitude of  $T_g$  depression in PS NPs and the matrix stiffness, as measured by the Debye-Waller factor.

### Role of Interfacial Interactions on $T_g$ Deviation of PS Nanoparticles

The PS NPs were prepared by surfactant free emulsion polymerization utilizing a persulfate chain initiator. The surfaces



of the NPs are negatively charged and have a zeta potential of approximately  $-40$  mV.<sup>42</sup> How each liquid interacts with the interface of PS could strongly influence interfacial glassy dynamics, and hence the  $T_g$ . The importance of the PS/liquid interface in determining the  $T_g$  of PS NPs has been demonstrated by the dramatic influence of a small addition of surfactants on the  $T_g$  of PS NPs dispersed in an aqueous medium. Zhu and coworkers illustrated that for PS NPs with  $d = 54$  nm, the  $T_g$ s were approximately 330 and 370 K, respectively, without a surfactant and with a 2 wt % (with respect to the polymer) addition of sodium dodecylbenzene sulfonate.<sup>49</sup> This observation is in qualitative agreement with prior literature studies, including those of Zhang.<sup>53</sup>

We illustrate the importance of interfacial interactions on the deviation in  $T_g$  of PS NPs via a solvent displacement study in which one liquid interface is displaced by another liquid interface. Water was used to displace either glycerol or [BMIM][CF<sub>3</sub>SO<sub>3</sub>] by re-suspending the NPs in water, which were formerly suspended in glycerol or [BMIM][CF<sub>3</sub>SO<sub>3</sub>]. The particles were washed via numerous cycles of centrifugation, re-suspension with water, and sonication until the suspension concentration of glycerol or [BMIM][CF<sub>3</sub>SO<sub>3</sub>] in water was approximately  $10^{-8}$  M. Subsequently, the  $T_g$  of nanoparticles dispersed in the aqueous environment was measured. The results are illustrated in Figure 3(A) for the case of PS particles with  $d \sim 428$  nm. Recall that  $T_g - T_{g,bulk} = -7$  K and  $-3$  K for PS particles with  $d \sim 428$  nm suspended in glycerol and the ionic liquid, respectively, as presented in Figure 2. Upon re-suspension in an aqueous medium, particles formerly dispersed in glycerol exhibited a  $-10$  K deviation in  $T_g$  with respect to  $T_{g,bulk}$ . The nanoparticles, therefore, exhibited a  $-3$  K shift in the particle  $T_g$  by changing the dispersing medium. Nanoparticles re-suspended in water from the ionic liquid exhibited the same  $-3$  K deviation in  $T_g$  with respect to  $T_{g,bulk}$  that was observed for particles suspended in the ionic liquid.

Hence, we observed a partial recovery of the  $T_g$  deviation of particles suspended in an aqueous environment when re-suspended from glycerol but no recovery of the  $T_g$  deviation for particles re-suspended from the ionic liquid. We argue that the partial recovery of  $T_g$  in transferring the NPs from glycerol to water is due to the partial displacement of the glycerol by water at the NP interface. The absence of any recovery in the  $T_g$  in transferring the NPs from [BMIM][CF<sub>3</sub>SO<sub>3</sub>] to water is due to the lack of displacement of the ionic liquid from the nanoparticle interface. Indeed, the presence of [BMIM][CF<sub>3</sub>SO<sub>3</sub>] on the surface of PS NPs after the re-suspension procedure was observed via XPS, as illustrated by Figure 3(B). These F 1s spectra probe composition within 9 nm of the surface. An XPS spectrum of particles re-suspended from glycerol was not collected as the acrylic acid present in the NPs has the same chemical constituents as glycerol. Our results illustrate that even the presence of a small amount of an additive that partitions to the nanoparticle/liquid interface can have a dramatic effect on the NP  $T_g$ , which is in agreement with the results of an ear-

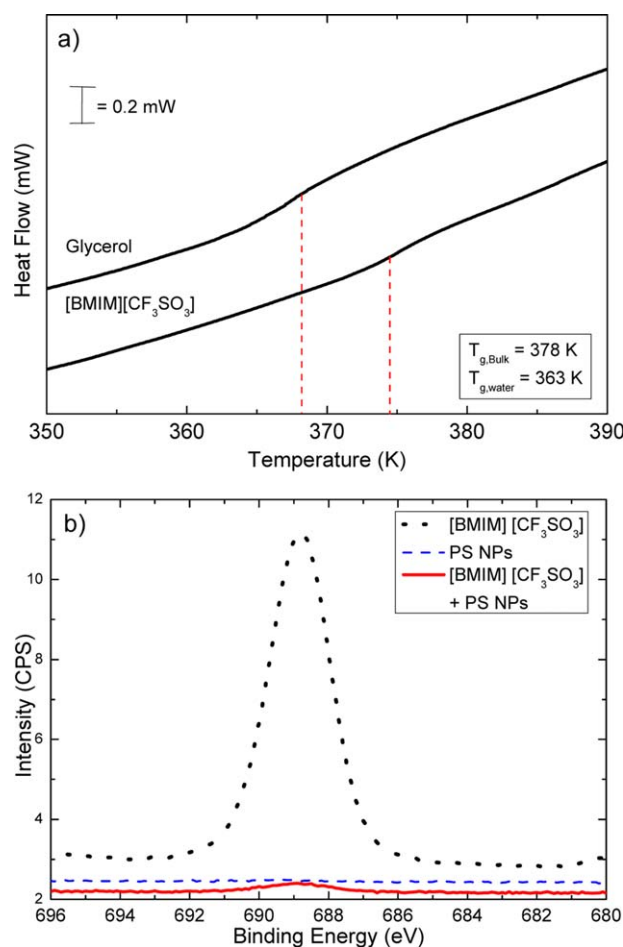


**FIGURE 3** (a) Calorimetric thermograms of PS NPs ( $d = 428$  nm) formerly suspended in glycerol or [BMIM][CF<sub>3</sub>SO<sub>3</sub>] re-suspended in water via dilution. The dashed lines represent the midpoint  $T_g$ s. The data are shifted for clarity. (b) XPS spectra obtained from [BMIM][CF<sub>3</sub>SO<sub>3</sub>], PS NPs, and PS NPs + [BMIM][CF<sub>3</sub>SO<sub>3</sub>] after re-suspension. All three curves are shown on the same scale. [Color figure can be viewed in the online issue, which is available at [wileyonlinelibrary.com](http://wileyonlinelibrary.com).]

lier work examining the influence of surfactant addition on the  $T_g$  of PS NPs.<sup>49</sup>

In an attempt to correlate interfacial interactions with the trend in  $T_g$  deviation observed for PS NPs suspended in various liquids, we computed the values of interfacial energy. The interfacial energy at the polymer/substrate interface has been previously correlated to  $T_g$  deviations in PS films supported on silicon and silicon-treated substrates.<sup>54</sup> Here, interfacial energies were calculated from Young's equation using surface tension and contact angle values from the literature and were found to be 7.25, 17.3, and 27.5 mJ/m<sup>2</sup> for [BMIM][CF<sub>3</sub>SO<sub>3</sub>], glycerol, and water, respectively. In order of increasing interfacial energy, [BMIM][CF<sub>3</sub>SO<sub>3</sub>]/PS < glycerol/PS < water/PS. This trend suggests a positive correlation between the surface energy and the magnitude of  $T_g$  deviations of the suspended PS NPs.

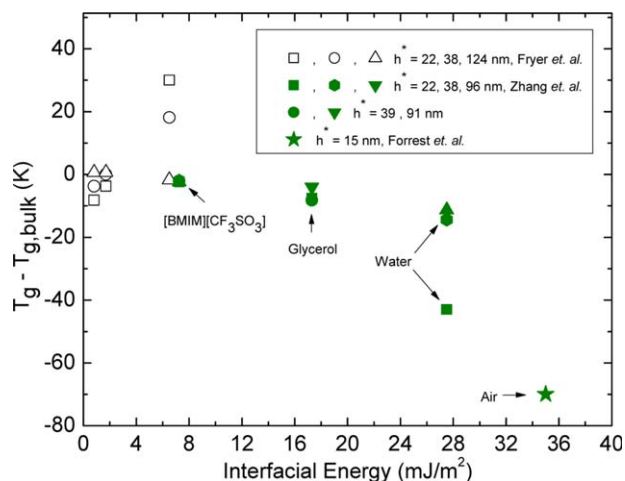


**FIGURE 4** Comparison of the dependence of the  $T_g$  shift on interfacial energy for PS thin films investigated by Fryer et al., Forrest et al., and PS NPs suspended in different liquid media. The characteristic length of the sphere ( $h^*$ ) is defined as the ratio of the sphere volume to surface area. [Color figure can be viewed in the online issue, which is available at [wileyonlinelibrary.com](http://wileyonlinelibrary.com).]

In Figure 4, we plot  $T_g - T_{g,bulk}$  (K) as a function of interfacial energy ( $\text{mJ}/\text{m}^2$ ) for PS NPs of various characteristic sizes ( $h^*$ ) defined as the volume to surface area ratio. Irrespective of NP diameter, no change in  $T_g$  is observed for particles dispersed in [BMIM][CF<sub>3</sub>SO<sub>3</sub>], that is, the low surface energy fluid. As the interfacial energy is increased between the fluid and PS, the influence of size on the magnitude of the  $T_g$  deviation is enhanced, as evident from the comparison presented in Figure 4. We also plot results from Fryer et al. on PS thin films supported on silicon-treated substrates.<sup>54</sup> The trend observed between the  $T_g$  deviation and interfacial energy for thin films is opposite from what is observed for dispersed PS NPs. However, for several reasons, caution should be taken when making this comparison. This is because nanoparticles dispersed in a liquid are exposed to only one interface while substrate-supported thin films are inherently exposed two interfaces, that is, the substrate and air interfaces. Competition between substrate and free surface interfacial effects in thin films, which are not fully understood, makes a direct comparison to dispersed NPs non-trivial. For instance, the interfacial energy of the PS/air interface is approximately  $35 \text{ mJ}/\text{m}^2$  and<sup>55</sup> is greater than that of the polymer-substrate interface. Yet, it is well documented that  $T_g$  is reduced at the air interface of PS.<sup>19</sup> In fact, the trend between  $T_g$  depressions with confinement and interfacial energy is strengthened when free standing films are considered, as illustrated in Figure 4. Another factor complicating the comparison, as alluded to in the preceding section, is the difference in the stiffness of the interfaces. Therefore, this comparison reveals that both the strength of the interfacial interactions as well as the rigidity of the interface plays an important role in determining the magnitude of  $T_g$  deviations in confined polymers. We note that Lang et al. has proposed an empirical expression aimed at capturing the influence of

these two factors on the  $T_g$  of confined polymer, though it has yet to be tested experimentally.<sup>52</sup>

### Comparison of $T_g$ Changes to Thin Films Floated Atop Liquid Substrates from Literature

Despite the difference in interfacial symmetry between nanoparticles and thin films, we compare our work to select studies that have measured  $T_g$  of thin films suspended atop similar liquids. In Figure 5, we plot the results from this investigation (open symbols) as a function of the characteristic length to allow for a comparison with literature results. In addition, we show results from McKenna et al.<sup>41</sup> for PS thin films suspended atop [BMIM][CF<sub>3</sub>SO<sub>3</sub>] and glycerol and those of Bodiguel and Fretigny<sup>39</sup> for films suspended atop of glycerol. Finally, we also include results from Lu et al.<sup>37</sup> of the “kink temperature” of PS thin films floated atop [BMIM][CF<sub>3</sub>SO<sub>3</sub>]. We note that McKenna et al. have reinterpreted the kink temperature as a devitrification temperature upon heating. The deviation in  $T_g$  as a function of characteristic length for PS NPs dispersed in glycerol is in qualitative agreement with the results of McKenna et al. and those of Bodiguel and Fretigny down to a characteristic length of approximately 20 nm. Below  $h^* \sim 20 \text{ nm}$ , McKenna et al. observe a dramatic decrease in  $T_g$ . Unfortunately, we are unable to probe  $T_g$  at similar length scales with nanoparticles.

In the case of PS NPs suspended in the ionic liquid, we observe little to no change in  $T_g$  as a function of characteristic size down to approximately 20 nm. Comparison with the work of Wang et al.<sup>41</sup> and the kink temperature of Lu et al.<sup>37</sup> shows good qualitative agreement in the  $T_g$  at the length scales of PS NPs that we are able to probe. It is not until  $h^* < 20 \text{ nm}$  that both studies show a significant size-dependent  $T_g$ . The qualitative agreement of our results with those of the literature, within the characteristic length scales probed, are interesting in lieu of the differences in the

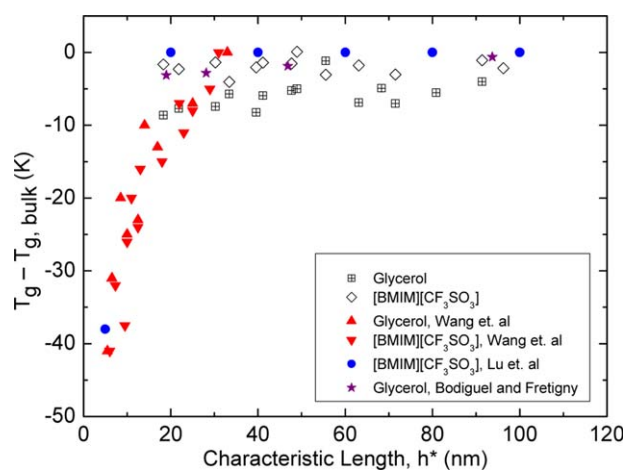


**FIGURE 5** Comparison of literature data on the influence of liquid media and size on  $T_g$  of PS thin films or NPs suspended on or in glycerol and [BMIM][CF<sub>3</sub>SO<sub>3</sub>], respectively. [Color figure can be viewed in the online issue, which is available at [wileyonlinelibrary.com](http://wileyonlinelibrary.com).]

interfaces, that is, symmetric versus asymmetric. However, all interfaces may be classified as “soft,” and therefore influence  $T_g$  in a similar manner. Further work in exploring the relative contributions of interfacial softness and rigidity on the size-dependent  $T_g$  is warranted.

## CONCLUSIONS

The influence of diameter on the  $T_g$  of PS NPs dispersed in either glycerol or [BMIM][CF<sub>3</sub>SO<sub>3</sub>] was investigated using DSC. Nanoparticles suspended in glycerol exhibited a weak diameter-dependence of  $T_g$  while those suspended in [BMIM][CF<sub>3</sub>SO<sub>3</sub>] showed no diameter-dependence of  $T_g$ . Nanoparticles re-suspended in an aqueous medium from glycerol exhibited a lower  $T_g$  than the former, while those re-suspended from [BMIM][CF<sub>3</sub>SO<sub>3</sub>] exhibited the same  $T_g$  in both media. We did not observe a correlation between the size-dependence of  $T_g$  and viscosity of the dispersing media for PS NPs. In contrast, a correlation between the size-dependence of  $T_g$  and interfacial energy was observed for the PS NPs. A comparison of our data with thin films (supported atop a liquid or solid substrate) revealed a non-trivial interplay between interfacial softness and interfacial interactions on the  $T_g$  of confined PS.

## ACKNOWLEDGMENTS

D.C. acknowledges support of a NSF Graduate Research Fellowship, while C.Z. acknowledges support of a NDSEG Research Fellowship. R.D.P. acknowledges support of the NSF Materials Research Science and Engineering Center program through the Princeton Center for Complex Materials (DMR-1420541).

## REFERENCES AND NOTES

- 1 T. G. Fox, P. J. Jr, Flory, *J. Appl. Phys.* **1950**, *21*, 581–591.
- 2 F. Karasz, W. MacKnight, *Macromolecules* **1968**, *1*, 537–540.
- 3 A. J. Kovacs, *J. Polym. Sci.* **1958**, *30*, 131–147.
- 4 J. Forrest, K. Dalnoki-Veress, J. Stevens, J. Dutcher, *Phys. Rev. Lett.* **1996**, *77*, 2002.
- 5 W. E. Wallace, J. H. Vanzanten, W. L. Wu, *Phys. Rev. E* **1995**, *52*, R3329–R3332.
- 6 K. Dalnoki-Veress, J. A. Forrest, C. Murray, C. Gigault, J. R. Dutcher, *Phys. Rev. E* **2001**, *63*, 031801.
- 7 J. Y. Park, G. B. McKenna, *Phys. Rev. B* **2000**, *61*, 6667–6676.
- 8 M. K. Mundra, C. J. Ellison, R. E. Behling, J. M. Torkelson, *Polymer* **2006**, *47*, 7747–7759.
- 9 E. Manias, V. Kuppa, D. K. Yang, D. B. Zax, *Colloids Surf. A* **2001**, *187*, 509–521.
- 10 A. Schonhals, H. Goering, C. Schick, B. Frick, R. Zorn, *Colloid Polym. Sci.* **2004**, *282*, 882–891.
- 11 M. Y. Efremov, A. V. Kiyanova, J. Last, S. S. Soofi, C. Thode, P. F. Nealey, *Phys. Rev. E* **2012**, *86*, 021501.
- 12 H. J. Yin, S. Napolitano, A. Schonhals, *Macromolecules* **2012**, *45*, 1652–1662.
- 13 C. J. Ellison, M. K. Mundra, J. M. Torkelson, *Macromolecules* **2005**, *38*, 1767–1778.
- 14 O. K. C. Tsui, H. F. Zhang, *Macromolecules* **2001**, *34*, 9139–9142.
- 15 J. L. Keddie, R. A. L. Jones, R. A. Cory, *Europhys. Lett.* **1994**, *27*, 59–64.
- 16 J. L. Keddie, R. A. L. Jones, R. A. Cory, *Faraday Discuss.* **1994**, *98*, 219–230.
- 17 K. Paeng, S. F. Swallen, M. D. Ediger, *J. Am. Chem. Soc.* **2011**, *133*, 8444–8447.
- 18 Y. Chai, T. Salez, J. D. McGraw, M. Benzaquen, K. Dalnoki-Veress, E. Raphael, J. A. Forrest, *Science* **2014**, *343*, 994–999.
- 19 C. J. Ellison, J. M. Torkelson, *Nat. Mater.* **2003**, *2*, 695–700.
- 20 G. B. DeMaggio, W. E. Frieze, D. W. Gidley, M. Zhu, H. A. Hristov, A. F. Yee, *Phys. Rev. Lett.* **1997**, *78*, 1524–1527.
- 21 C. B. Roth, J. R. Dutcher, *J. Electroanal. Chem.* **2005**, *584*, 13–22.
- 22 M. D. Ediger, J. A. Forrest, *Macromolecules* **2014**, *47*, 471–478.
- 23 J. A. Forrest, K. Dalnoki-Veress, *Adv. Colloid Interf. Sci.* **2001**, *94*, 167–196.
- 24 J. H. Kim, J. Jang, W. C. Zin, *Langmuir* **2001**, *17*, 2703–2710.
- 25 J. S. Sharp, J. A. Forrest, *Phys. Rev. Lett.* **2003**, *91*, 235701.
- 26 S. Peter, H. Meyer, J. Baschnagel, *J. Polym. Sci. Part B: Polym. Phys.* **2006**, *44*, 2951–2967.
- 27 Z. H. Yang, Y. Fujii, F. K. Lee, C. H. Lam, O. K. C. Tsui, *Science* **2010**, *328*, 1676–1679.
- 28 D. S. Fryer, P. F. Nealey, J. J. de Pablo, *Macromolecules* **2000**, *33*, 6439–6447.
- 29 R. D. Priestley, M. K. Mundra, N. J. Barnett, L. J. Broadbelt, J. M. Torkelson, *Aust. J. Chem.* **2007**, *60*, 765–771.
- 30 Y. Grohens, M. Brogly, C. Labbe, M. O. David, J. Schultz, *Langmuir* **1998**, *14*, 2929–2932.
- 31 Y. Grohens, L. Hamon, G. Reiter, A. Soldera, Y. Holl, *Eur. Phys. J. E* **2002**, *8*, 217–224.
- 32 C. E. Porter, F. D. Blum, *Macromolecules* **2000**, *33*, 7016–7020.
- 33 G. Vignaud, J. F. Bardeau, A. Gibaud, Y. Grohens, *Langmuir* **2005**, *21*, 8601–8604.
- 34 C. B. Roth, J. R. Dutcher, *Eur. Phys. J. E* **2003**, *12*, S103–S107.
- 35 J. A. Forrest, K. Dalnoki-Veress, J. R. Dutcher, *Phys. Rev. E* **1997**, *56*, 5705–5716.
- 36 P. Rittigstein, R. D. Priestley, L. J. Broadbelt, J. M. Torkelson, *Nat. Mater.* **2007**, *6*, 278–282.
- 37 H. Y. Lu, W. Chen, T. P. Russell, *Macromolecules* **2009**, *42*, 9111–9117.
- 38 J. H. Wang, G. B. McKenna, *Macromolecules* **2013**, *46*, 2485–2495.
- 39 H. Bodiguel, C. Fretigny, *Macromolecules* **2007**, *40*, 7291–7298.
- 40 J. H. Wang, G. B. McKenna, *J. Polym. Sci. Part B: Polym. Phys.* **2013**, *51*, 1343–1349.
- 41 J. H. Wang, G. B. McKenna, *Macromolecules* **2013**, *46*, 3698–3698.
- 42 C. Zhang, Y. L. Guo, R. D. Priestley, *Macromolecules* **2011**, *44*, 4001–4006.
- 43 C. Zhang, Y. L. Guo, R. D. Priestley, *J. Polym. Sci. Part B: Polym. Phys.* **2013**, *51*, 574–586.
- 44 L. Zhang, M. D’Acunzi, M. Kappl, G. K. Auernhammer, D. Vollmer, C. M. van Kats, A. van Blaaderen, *Langmuir* **2009**, *25*, 2711–2717.
- 45 C. Zhang, V. J. Pansare, R. K. Prud’homme, R. D. Priestley, *Soft Matter* **2012**, *8*, 86–93.
- 46 C. Zhang, J. W. Chung, R. D. Priestley, *Macromol. Rapid Commun.* **2012**, *33*, 1798–1803.

- 47** C. Zhang, V. M. Boucher, D. Cangialosi, R. D. Priestley, *Polymer* **2013**, *54*, 230–235.
- 48** L. D. Feng, X. C. Bian, G. Li, Z. M. Chen, Y. Cui, X. S. Chen, *Polym. Test.* **2013**, *32*, 1368–1372.
- 49** S. Feng, Z. Y. Li, R. Liu, B. Y. Mai, Q. Wu, G. D. Liang, H. Y. Gao, F. M. Zhu, *Soft Matter* **2013**, *9*, 4614–4620.
- 50** Y. Rharbi, *Phys. Rev. E* **2008**, *77*, 031806.
- 51** C. B. Roth, J. M. Torkelson, *Macromolecules* **2007**, *40*, 3328–3336.
- 52** R. J. Lang, W. L. Merling, D. S. Simmons, *Acs Macro Lett.* **2014**, *3*, 758–762.
- 53** C. Zhang, Size and interfacial effects on the glass transition and associated dynamics in nanoscopically-confined polymer glasses, 2014, Princeton University.
- 54** D. S. Fryer, R. D. Peters, E. J. Kim, J. E. Tomaszewski, J. J. de Pablo, P. F. Nealey, C. C. White, W. L. Wu, *Macromolecules* **2001**, *34*, 5627–5634.
- 55** S. Wu, *J. Phys. Chem.* **1968**, *72*, 3332–3334.